We may solve this problem numerically (assuming a value for N and m_h) by finding the value of E_F which makes the integrals equal. This was done by computer, assuming $m_h=0.1m$ (the crystalline value) and choosing two values of N corresponding to a total "impurity" concentration of 10^{18} and 10^{19} cm^{-3}. This is determined simply by

$$\text{total impurity concentration}=\int_0^\infty Ne^{-E/0.14}dE. \quad \text{(A6)}$$

Five values of temperature were used, ranging from 290 to 58°K. The results are shown in Fig. 6.

PHYSICAL REVIEW VOLUME 154, NUMBER 3 15 FEBRUARY 1967

p-Type Photoelectric Behavior in CdS Dominated by a High-Resistivity Region near the Anode*

K. W. Böer and J. J. Ward
Physics Department, University of Delaware, Newark, Delaware
(Received 22 August 1966)

It is observed, using the Franz-Keldysh effect, that certain very pure CdS crystals show a high-field layer close to, but well separated from, a hole-injecting anode (Au). Inversion of an infrared quenching spectrum into a similar infrared excitation spectrum is observed at an applied voltage where this high-field layer becomes "visible." The data are tentatively interpreted in terms of a model with a current-controlling p-type region adjacent to the anode and produced by hole injection, followed by a p-n junction identified with the observed high-field region, followed by the normal n-type region occupying most of the bulk.

I. INTRODUCTION

CADMIUM sulfide at room temperature has always been observed to be n type,[1–6] and it is not yet possible to dope CdS in such a way that it becomes p type. However, there are some indications that the ratio of hole to electron concentration in CdS can be increased by injection of holes from the anode. The observation of green electroluminescence has been attributed to such an injection mechanism.[7–10] If this injection is strong enough, one may obtain regions of the crystal with predominant hole concentration close to the anode. The material here can become p type. In this region, the electron density is strongly reduced because of an enhanced recombination. In a transition region between n-type and p-type material, the lowest carrier concentration will be observed. This region will act essentially as a p-n junction caused by a minority-carrier injection and will present a layer of highest resistivity, and thereby highest field strength, in the crystal. Under certain conditions, this junction may control the current through the crystal.

There exist some theoretical investigations into similar double-injection phenomena which show that characteristic deviations of the current-voltage characteristic occur when the injection becomes marked.[11,12]

However, up to now, there was no direct experimental evidence for such a single-injection-produced p-n junction. Therefore, the Franz-Keldysh effect[13,14] has been used to look for these high-field layers associated with the p-n junction. After observing such layers in certain crystals, the influence of visible and infrared illumination and applied voltage was studied. The results of this work are reported in this paper.

II. EXPERIMENTAL METHOD

Thin CdS single-crystal platelets, grown by sublimation in an N_2–H_2S atmosphere at about 1100°C, were prepared with evaporated Au electrodes, covered with an evaporated film of Cr (for mechanical protection). The electrodes were deposited at a pressure of 10^{-6} Torr onto opposite sides of the crystal with a spacing of about 1.5 mm. Any heat treatment which

* Work sponsored by the Office of Naval Research, Washington, D. C., Contract No. NONR(G) 4336-(00).

[1] p-type conductivity in heavily Cu-treated CdS reported earlier (Refs. 2, 3) has recently been shown (Refs 4–6) to be due to precipitation of copper compounds and cannot be attributed to CdS.

[2] J. Woods and J. A. Champion, J. Electron. Control **7**, 243 (1959).

[3] D. C. Reynolds, L. C. Green, R. G. Wheeler, and R. S. Hogan, Bull. Am. Phys. Soc. **3**, 111 (1956).

[4] A. Dreeben, J. Electrochem. Soc. **111**, 174 (1964).

[5] N. I. Vitrikhovskii and M. V. Kurik, Fiz. Tver. Tela **7**, 3676 (1965) [English transl.: Soviet Phys.—Solid State **7**, 2969 (1966).

[6] H. Sturner and C. E. Bleil, Appl. Opt. **3**, 1015 (1964).

[7] R. Smith, Phys. Rev. **105**, 900 (1957).

[8] K. W. Böer, H. J. Hänsch, and H. Obernik, Phys. Status Solidi **1**, 352 (1961).

[9] H. Yamashita, S. Ibuki, M. Yoshizawa, and H. Komiya, J. Phys. Soc. Japan **15**, 2366 (1960).

[10] G. Diemer, Phillips Res. Rept. **9**, 109 (1954).

[11] M. A. Lampert, Phys. Rev. **125**, 126 (1962).

[12] C. W. Litton and D. C. Reynolds, Phys. Rev. **133**, A536 (1964).

[13] W. Franz, Z. Naturforsch. **13a**, 484 (1958).

[14] I. V. Keldysh, Zh. Eksperim. i Teor. Fiz. **34**, 1138 (1958) [English transl.: Soviet Phys—JETP **6**, 788 (1958)].

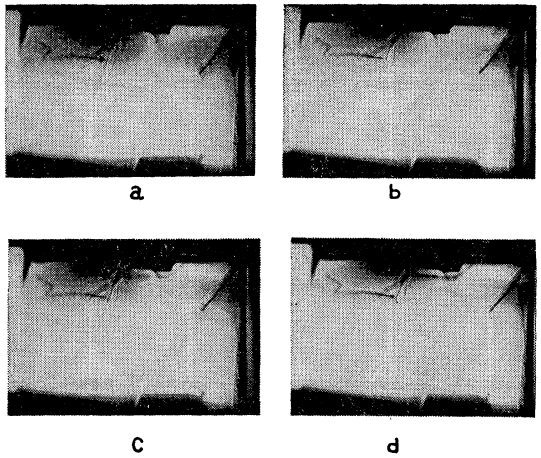

FIG. 1. Photographs of CdS crystals in near-band-edge monochromatic light: $\lambda = 515$ mμ, T = 300°K. The upper electrode is the anode. The "ring" around the anode in (b)–(d) indicates the high-field layer (best visible below the right half of the anode; the odd-shaped line extending further into the crystal below the left half of the anode is a crystal defect). Applied voltage: (a) 0 V, (b) 300 V, (c) 750 V, and (d) 1250 V.

would allow diffusion of the electrode metal into the CdS was carefully avoided.

The crystals were kept in a high-purity N_2 atmosphere during all measurements. They were mounted in the bore of a copper block for temperature variation, and could be irradiated using a tungsten lamp in conjunction with a Leitz double-prism monochromator. Spatial inhomogeneities in the optical transmission spectrum could be directly observed and photographed. Additional infrared light was supplied, using a Bausch and Lomb grating monochromator or a tungsten source with infrared (IR) band pass filters and a fiber optics. For light attenuation, a calibrated set of Wratten gray filters was used. The applied voltage was supplied

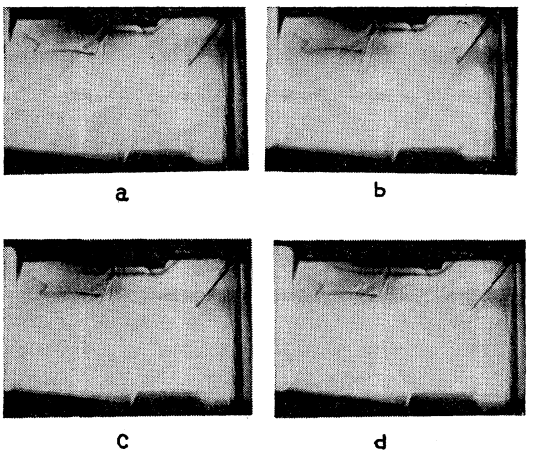

FIG. 2. Photographs of CdS crystals as in Fig. 1 at 1250-V applied voltage, taken at different additional infrared intensities I: (a) same conditions as in Fig. 1(d); $I = I_0$. (b) $I = 10I_0$. (c) $I = 100I_0$. (d) $I = 1000I_0$. (Broad band IR irradiation: 0.85 to 2.0 μ.)

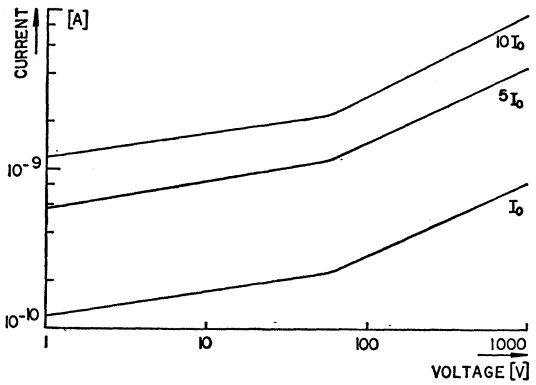

FIG. 3. Current-voltage characteristics (excitation with 515 mμ, $I_0 = 3 \times 10^{12}$ photons/cm^2 sec).

from a variable dc power supply. The current was measured with a Keithley 415 picoammeter and recorded with a Houston Instrument HR 96T x-y recorder. For breakdown protection, a 1-MΩ series resistor was used.

III. EXPERIMENTAL RESULTS

A. Electro-Optical Investigations

With increased applied voltage two types of field inhomogeneities are usually observed[15] using the elector-optical method: barrier layers at the electrodes,[16] and, at higher voltages, characteristic layer-like field inhomogeneities caused by negative differential conductivity as described earlier.[17,18]

The first type will not be discussed further in this paper. Layer-like field inhomogeneities are usually created near the cathode, and, at high enough applied voltages, start to move through the crystal towards the anode, where they disappear. A new layer forms at the cathode, and this cycle is repeated periodically.[17] In more inhomogeneously doped CdS crystals, these field inhomogeneities can also appear at various places of high defect density in the crystal. Often the field layers can be trapped at visible macroscopic crystal defects.[19] The behavior of these high-field layers has been reported in several earlier papers.[17–21] Their main properties, which allow them to be distinguished from other field inhomogeneities reported here, are: (a) the layer width increases in proportion to the increase in

[15] High-field regions are directly observable under monochromatic illumination close to the band edge as regions of increased absorption which appear darker than the remainder of the crystal in transparency observation. This is caused by the shift of the absorption edge towards longer wavelengths with increased electric field (Franz-Keldysh effect).

[16] K. W. Böer and U. Kümmel, Z. Physik. Chem. (Leipzig) **214**, 127 (1960).

[17] K. W. Böer, H. J. Hänsch, and U. Kümmel, Z. Physik **155**, 170 (1959).

[18] K. W. Böer, Phys. Rev. **139**, A1949 (1965).

[19] K. W. Böer and W. E. Wilhelm, Phys. Status Solidi **4**, 237 (1964).

[20] K. W. Böer, Z. Physik **155**, 184 (1959).

[21] K. W. Böer and R. Rompe, Ann. Physik **5**, 200 (1960).

the applied voltage, (b) the field strength within the layer is independent of the applied voltage, and (c) the layers tend to disappear with intense infrared illumination.

In certain very pure CdS crystals,[22] if the applied voltage is high enough, a new type of field inhomogeneity is observed, consisting of a narrow region of high field strength surrounding but well separated from the anode (Fig. 1). With increased applied voltage the field in the layer increases, but both the position of the layer and its width remain essentially constant [Figs. 1(b)–1(d)]. These layers are already observable at applied voltages as low as 100 V (1.5 mm electrode gap), i.e., at considerably lower values than those necessary for initiation of layer-like field inhomogeneities as described earlier (usually above 1000 V for similar electrode configuration).[17] As the infrared illumination is increased further,[23] the high-field region becomes more and more pronounced [Figs. 2(a)–2(d)].

The current-voltage characteristic is non-Ohmic and shows a pronounced sublinear behavior. From below 1 V to about 50 V it follows a power law with a slope of about 0.15; from 50 V to at least 1400 V—a value about 60% of the breakdown voltage—it follows a power law with a slope of about 0.5 (see Fig. 3). At applied voltages above which the high-field layer can be observed, the photoresponse time of the crystals is markedly reduced.

At 1400 V some portions of the high-field region become unstable (flickering appearance) without observable movement. This was also observed at somewhat lower applied voltages (about 1200 V) with intense additional infrared illumination. This instability occurs most easily in high-field regions in front of electrode corners (upper right electrode edge in Figs. 1 and 2). From visual electro-optical observations it appears to be

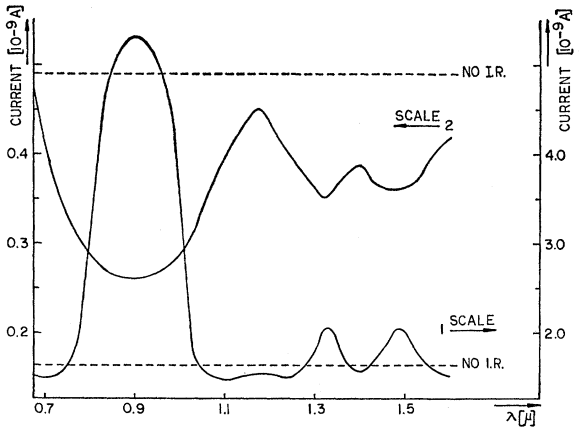

FIG. 4. Photocurrent (excitation with 515 mμ, 1.6×10^{12} photons/cm² sec) as a function of the wavelength of additional infrared excitation (excitation density given in the insert of Fig. 6). Applied voltage: (1) 1000 V, (2) 50 V.

[22] No impurities are detectable by spectrographic analysis.
[23] $I_0=6.5\ \mu W/cm^2$ in a range of 0.85 to 2 μ.

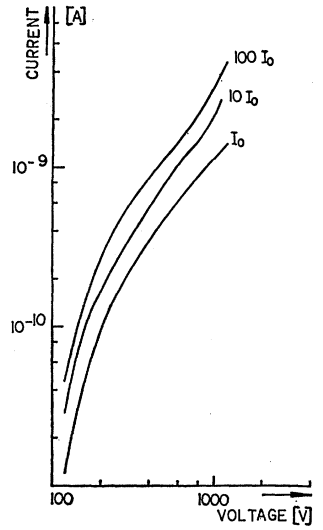

FIG. 5. Current-voltage characteristics for photoconductance excited by IR (only). Broad-band irradiation as in Fig. 2.

caused by a tendency for current channels to form through these regions.[24] High-current fluctuations are observed simultaneously. Green electroluminescence is observed after an electric breakdown of this high-field layer has occurred (it is not observable with adapted eyes below this punchthrough).

B. Infrared Quenching and Excitation Spectrum

At lower applied voltages (50 V for Fig. 4), the photocurrent shows the well-known quenching spectrum dur-

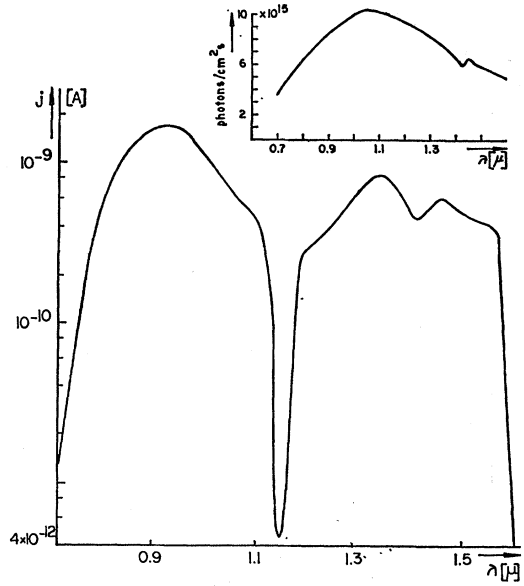

FIG. 6. Spectral distribution of the photoconductivity excited by IR (only) at an applied voltage of 900 V.

[24] K. W. Böer, H. J. Hänsch, U. Kümmel, H. Lange, and E. Nebauer, Phys. Status Solidi 1, 169 (1961).

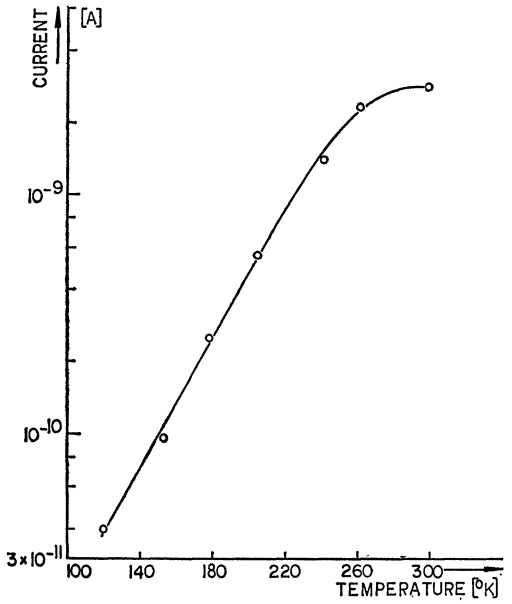

FIG. 7. Photoconductance excited by IR (only) as a function of temperature. Excitation with 925 mμ, 9×10^{15} photons/cm² sec; applied voltage 1000 V.

ing irradiation with additional infrared light (two-beam method).[25,26] Three current minima are observed, located at about 0.9, 1.33, and 1.48 μ. Here maximum quenching takes place. With increased applied voltage the quenching decreases, and at high enough voltages infrared excitation is observed instead (1000 V in Fig. 4). It should be noted that the "excitation spectrum" at higher voltages is essentially a mirror image of the "quenching spectrum" at lower voltages, i.e., the excitation maxima lie at the same wavelengths as the current minima for quenching. (Similar results were observed recently by Kitamura, Kubo, and Yamashita.[27]) In addition, at wavelengths between the "excitation maxima"—where at low applied voltages only negligible quenching occurs—now, at high applied voltages, the photocurrent decreases below the current value measured without additional infrared illumination. These new "high-voltage quenching" maxima lie at 0.7, 1.1, 1.24, 1.4, and above 1.6 μ.

Without primary beam (515 mμ) excitation, infrared photoconductivity[28] of these crystals can be observed for applied voltages above about 100 V and increases very steeply with increasing voltage (Fig. 5). The spectral distribution of the photoexcitation in the infrared range is given in Fig. 6 for an applied voltage of 900 V. It shows the abovementioned excitation maxima, a very pronounced excitation minimum at about 1.15 μ, and a steep cutoff at about 1.6 μ. The infrared photoconductivity, measured for excitation with 0.93 μ, increases with increasing temperature (as shown in Fig. 7). However, no simple exponential law is observed.

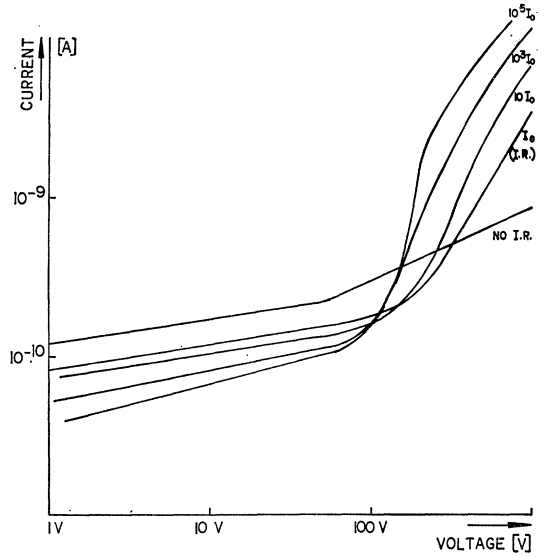

FIG. 8. Current-voltage characteristics for visible-light excitation 515 mμ, 3×10^{12} photons/cm² sec, and additional broad-band IR excitation as in Fig. 2.

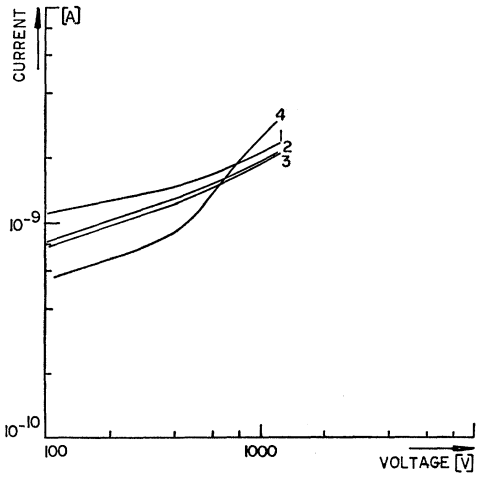

FIG. 9. Current-voltage characteristics for two-beam excitation: 515 mμ, 1.2×10^{13} photons/cm² sec and: (1) no IR, (2) 1.45 μ, (3) 1.35 μ, and (4) 925 mμ. The IR photon density was 8×10^{15} photons/cm² sec.

C. Current-Voltage Characteristic with Additional Infrared Irradiation

For low applied voltages, the current-voltage characteristic is essentially shifted downwards with increased additional infrared illumination (broad-band excitation 0.85 to 2 μ) as shown in Fig. 8. At high applied voltage, the current increase becomes steeper with

[25] R. Frerichs, Naturwiss. 33, 281 (1946).
[26] R. H. Bube, Phys. Rev. 99, 1105 (1955).
[27] S. Kitamura, T. Kubo, and T. Yamashita, J. Phys. Soc. Japan 16, 351 (1961).
[28] E. Schnürer, Phys. Status Solidi 6, 133 (1964).

higher infrared illumination, and, above 400 V, shows a typical infrared excitation behavior, i.e., it lies above the current observed with visible excitation only. The crossover point shifts towards lower voltages with increased infrared intensity. With increased visible light intensity, the crossover points between quenching and infrared excitation shift towards higher applied voltage, following a slightly steeper than linear law. The relative influence of the additional infrared decreases, and the deviations from the curve with visible excitation become more symmetric in the quenched and the infrared-excited range.

With additional monochromatic infrared irradiation, it is seen that the 0.93-μ irradiation changes from quenching to excitation at considerably lower applied voltages than the 1.35- or 1.45-μ irradiation (see Fig. 9).

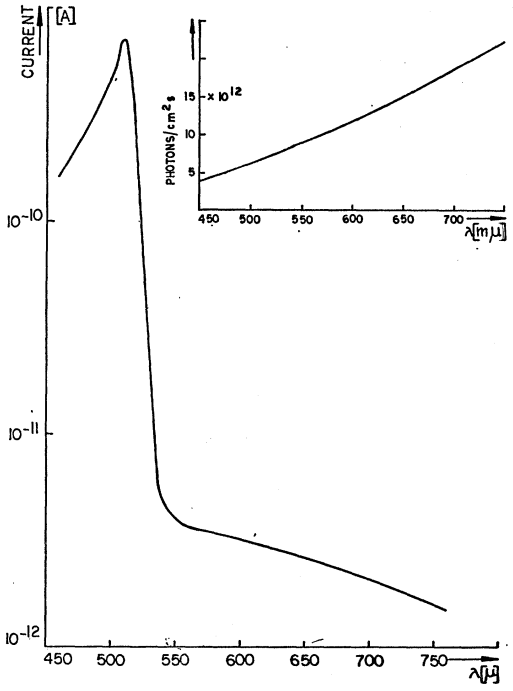

FIG. 10. Spectral distribution of photocurrent (density of incident photons as given in the insert of the figure). Applied voltage 10 V.

D. Defect Level Analysis

Crystals which show the described high-field layers near the anode show a spectral distribution of the photocurrent as given in Fig. 10. The steep decrease of the photocurrent over two orders of magnitude at the band edge (extrinsic range) indicates a relatively low density of hole traps close to the valence band. The estimated lifetime of electrons at the photoconductivity maximum (which lies at a wavelength such that about 80% of 6×10^{12} incident photons/cm^2 sec are absorbed) is $\tau\simeq6\times10^{-6}$ sec.

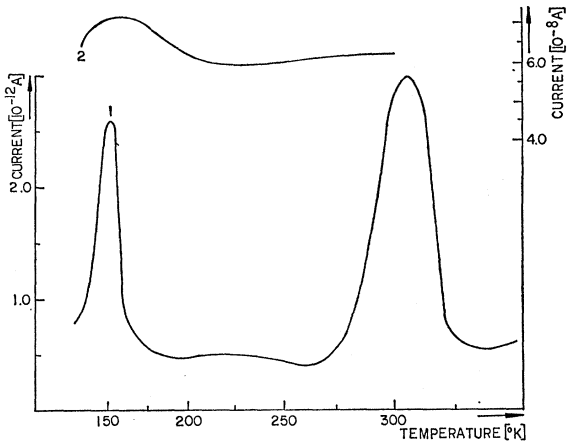

FIG. 11. Thermally stimulated current after 10-min excitation at 100°K (curve 1, left scale), and photocurrent as a function of the temperature (curve 2, right scale). (Excitation: white light, 25 ft-c.)

The thermally stimulated current curve (Fig. 11, curve 1) shows maxima at 150 and 300°K. Using $N_t=\int$jdt$/eGV_0$ where the gain factor $G=\tau\mu V/l^2$, and V_0 is the volume of the crystal between the electrodes, the estimated trap densities (taking $\mu=300$ cm^2/V sec, the lifetime for the photocurrent maximum and $V=10$ V) are $N_t(E_c-E_t=0.32\text{ eV})\simeq2\times10^{13}$ cm^{-3} and $N_t(E_c-E_t=0.65\text{eV})\simeq4\times10^{13}$ cm^{-3}. The use of the same lifetime is justified by the fact that essentially no thermal quenching is observed between room temperature and 150°K, as shown in Fig. 11, curve 2.

IV. DISCUSSION

In a certain type of undoped ("very pure") CdS single crystal, which shows a low density of hole traps close to the valence band and less than 10^{14} cm^{-3} electron traps in the range between 0.3 and 0.65 eV from the conduction band, characteristic high-field layers close to, but well separated from, the anode are ob-

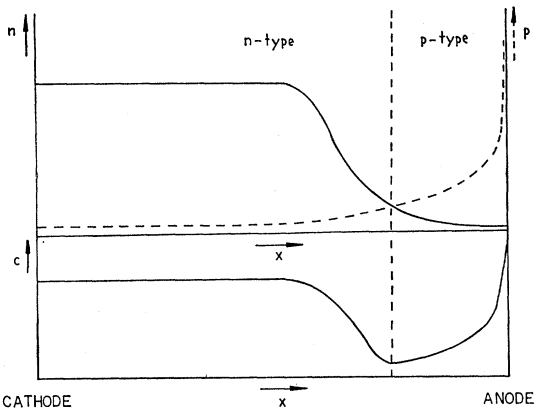

FIG. 12. Schematic plot of the electron and hole density as a function of the spatial coordinate between cathode and anode (upper part) and of the total carrier density (lower part).

served. These layers occur at high enough applied voltages and can be observed, using the Franz-Keldysh effect, above about 100 V. As these layers appear, a tendency for inversion from infrared quenching to infrared excitation and vice versa is observed. At high enough applied voltages and high enough infrared intensity, this inversion is fully developed.

These results suggest that hole injection from the anode becomes a predominant factor for photoconductance of these crystals and that the photocurrent is essentially determined by a crystal region with p-type character. Such regions can be obtained close to the anode, where a high hole concentration exists, because of injection from the hole-injecting contact (Au). Here the electron density decreases markedly because of strongly enhanced recombination with holes. This can proceed to a point where the hole concentration surpasses the electron concentration. Since the hole mobility ($\mu_p \simeq 20$ cm^2/V sec at room temperature) is considerably smaller than the electron mobility, and the density of free carriers is markedly reduced because of enhanced recombination, the conductivity in the region of predominant hole current must be much lower than in the n-type region of the remainder of the crystal.

In contrast to the case of double injection, the concentration of conduction electrons decreases monotonically from cathode to anode, and the highest recombination traffic takes place in a region directly adjacent to the anode.[29] Although the minimum carrier density c is observed in the p-n junction (see Fig. 12), the current through the crystal may be determined by the p-type region rather than by the resistance of the junction, if the p-type region is thick enough—since here, as mentioned above, the carrier density is strongly reduced by enhanced recombination (and $\mu_p < \mu_n$). Nevertheless the highest field strength occurs in the p-n junction, and this region can consequently be observed by means of electro-optical effects.

This therefore suggests that high-field layers close to a hole-injecting anode (e.g. Au, Cu), as very generally observed (e.g., by potential probing), are such single-injection-caused p-n junctions. However, only in crystals with a long hole lifetime can the p-n junction be separated from the anode by a long enough distance that the resistance of the p-type region becomes comparable to the resistance of the remainder of the crystal and influences its photoconductive properties. If this is the case, the infrared properties will tend to invert. The production of holes in a p-type region increases its conductivity, and the production of conduction electrons there increases the probability for recombination of holes, and therefore causes quenching, decreasing the conductivity of the p-type region. With additional infrared excitation the conductivity in the p-type region increases and the field here decreases, causing the field in the junction to increase, as is observed.

A quantitative discussion will be published in a theoretical paper currently in preparation.

[29] The fact that no luminescence was observed before punch-through of the p-n junction seems to indicate that these crystals have sufficient recombination centers for radiationless recombination.

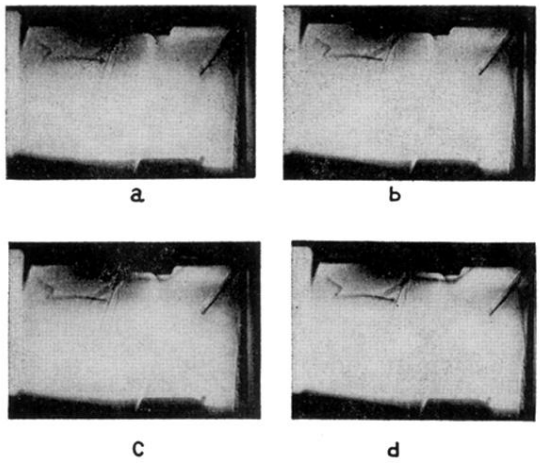

FIG. 1. Photographs of CdS crystals in near-band-edge monochromatic light: $\lambda = 515$ mμ, $T = 300°K$. The upper electrode is the anode. The "ring" around the anode in (b)–(d) indicates the high-field layer (best visible below the right half of the anode; the odd-shaped line extending further into the crystal below the left half of the anode is a crystal defect). Applied voltage: (a) 0 V, (b) 300 V, (c) 750 V, and (d) 1250 V.

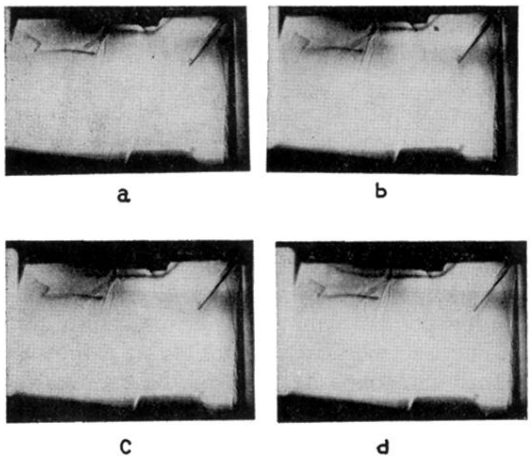

FIG. 2. Photographs of CdS crystals as in Fig. 1 at 1250-V applied voltage, taken at different additional infrared intensities I: (a) same conditions as in Fig. 1(d); $I = I_0$. (b) $I = 10I_0$. (c) $I = 100I_0$. (d) $I = 1000I_0$. (Broad band IR irradiation: 0.85 to 2.0 μ.)